Field theoretical methods in fluid and plasma theory

Florin Spineanu
National Institute of Laser, Plasma and Radiation Physics
Bucharest, Romania

In collaboration with Madalina Vlad

Objective: to develop a field-theoretical model that can provide a description of the $2D$ fluids close to stationarity.

The theory is relevant for the classical debate on the relation between

(1) large-scale organized, quasi-coherent flows, and

(2) "structures" (solitons, vortices, etc.)

Content

- The $2D$ discrete systems and the field theory formalism
- $2D$ water
- planetary atmosphere ($2D$ quasi-geostrophic)
  - tropical cyclone; relationships v_{θ}^{max}, R_{max}, $r_{v_{\theta}^{max}}$
- plasma (coherent) flows; crystals of vortices in non-neutral plasmas
- Related subjects: Concentration of vorticity; Contour Dynamics; statistics of turbulence; etc.

Main idea : there exist *preferred states* of the system.
The system makes transitions between these states.

Quasi-coherent structures are observed in

- fluids (in oceans and in laboratory experiments)
- plasma (confined in strong magnetic field)
- planetary atmosphere ($2D$ quasi-geostrophic)
- non-neutral plasma (crystals of vortices)

There are common features suggesting to develop models based on the self-organization of the vorticity field. The fluids evolve at relaxation precisely to a subset of stationary states.

It is found that besides *conservation* there is also *action*

Coherent structures in fluids and plasmas (reality)

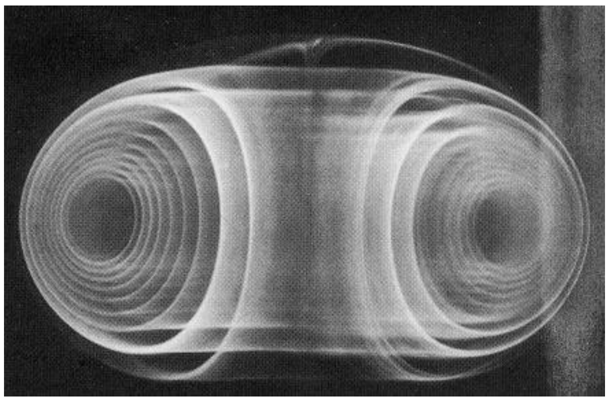

Rings of vorticity (Leonard 1998)

Nice tornado vortex.

Vortex ring emitted by the volcano Etna.

Coherent structures in fluids and plasmas (numerical 1)

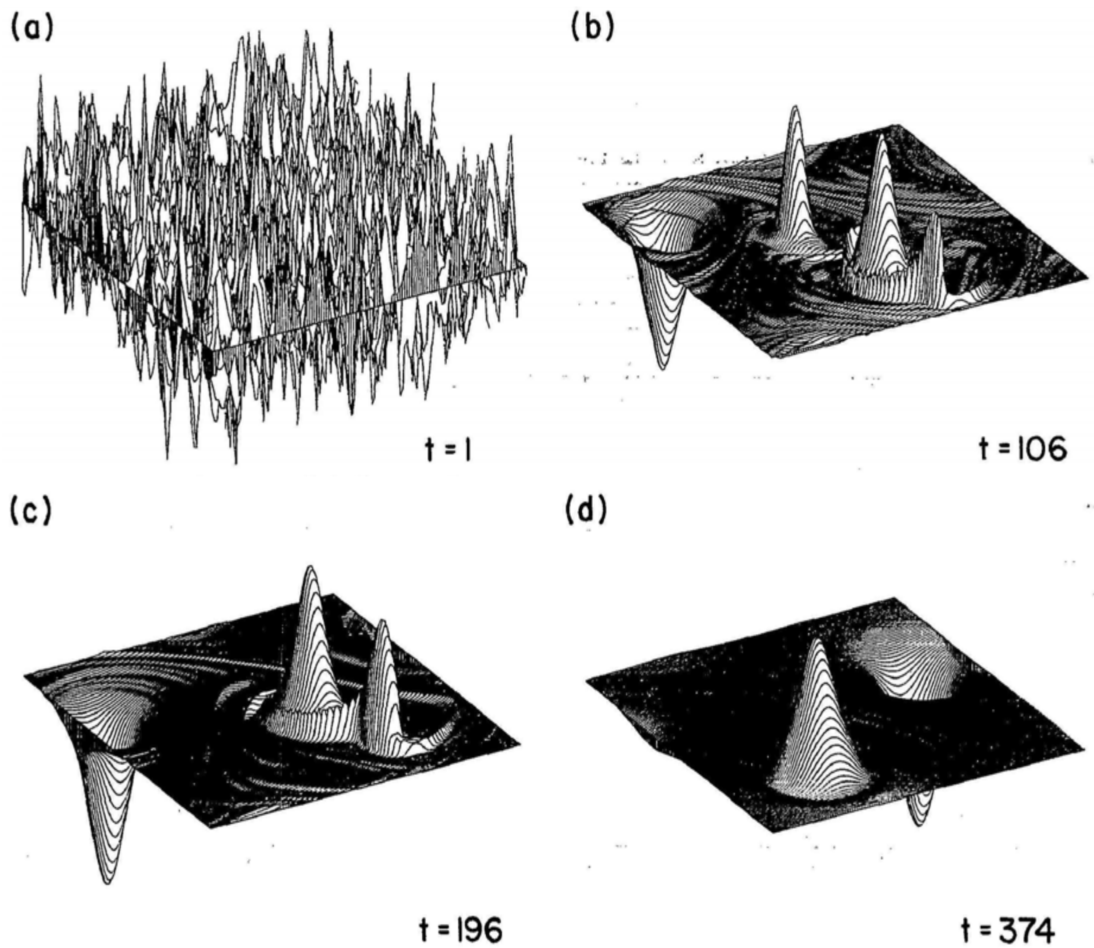

Numerical simulations of the Euler equation.

D. Montgomery, W.H. Matthaeus, D. Martinez, S. Oughton, Phys. Fluids A4 (1992) 3.

Coherent structures in fluids and plasmas (numerical 2)

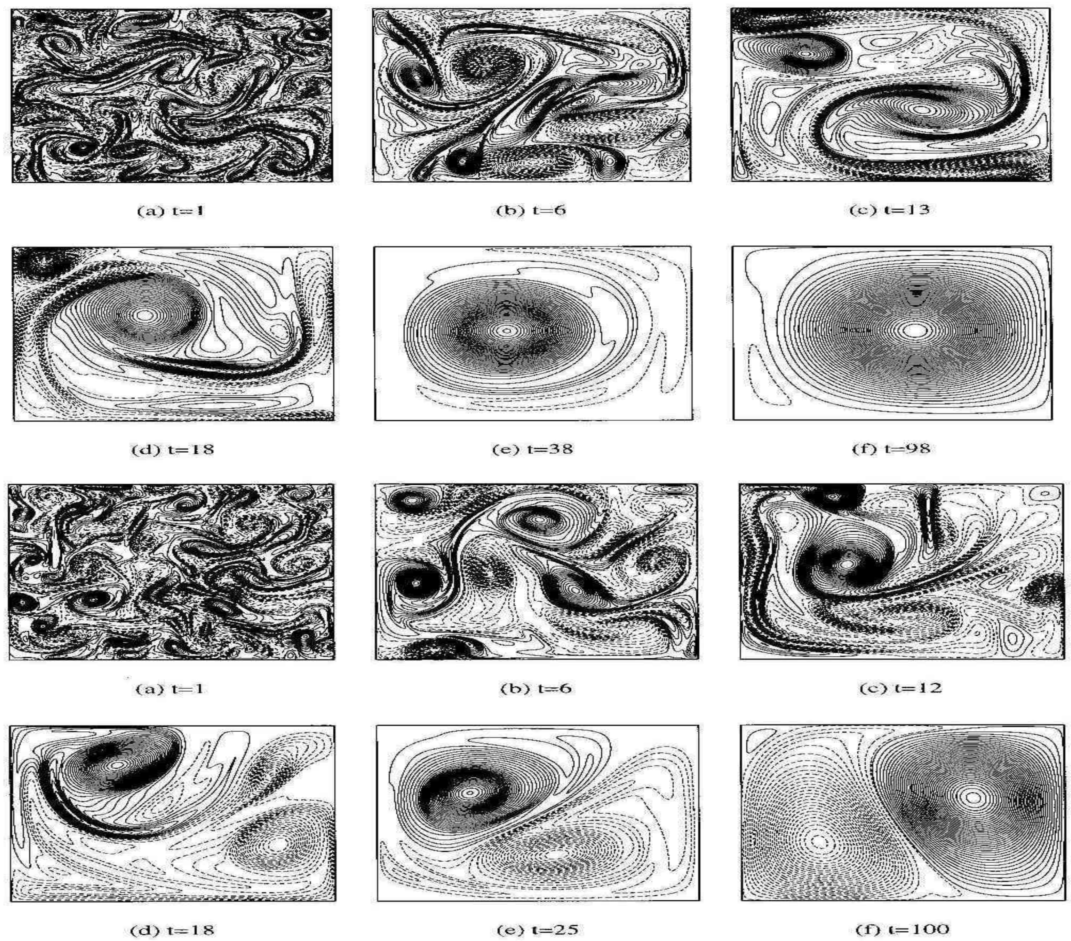

Numerical simulations of the Navier-Stokes equation.

H. Brands, S. R. Maasen, H.J.H. Clercx
Phys. Rev. E 60.

Coherent structures in fluids and plasmas (numerical 3)

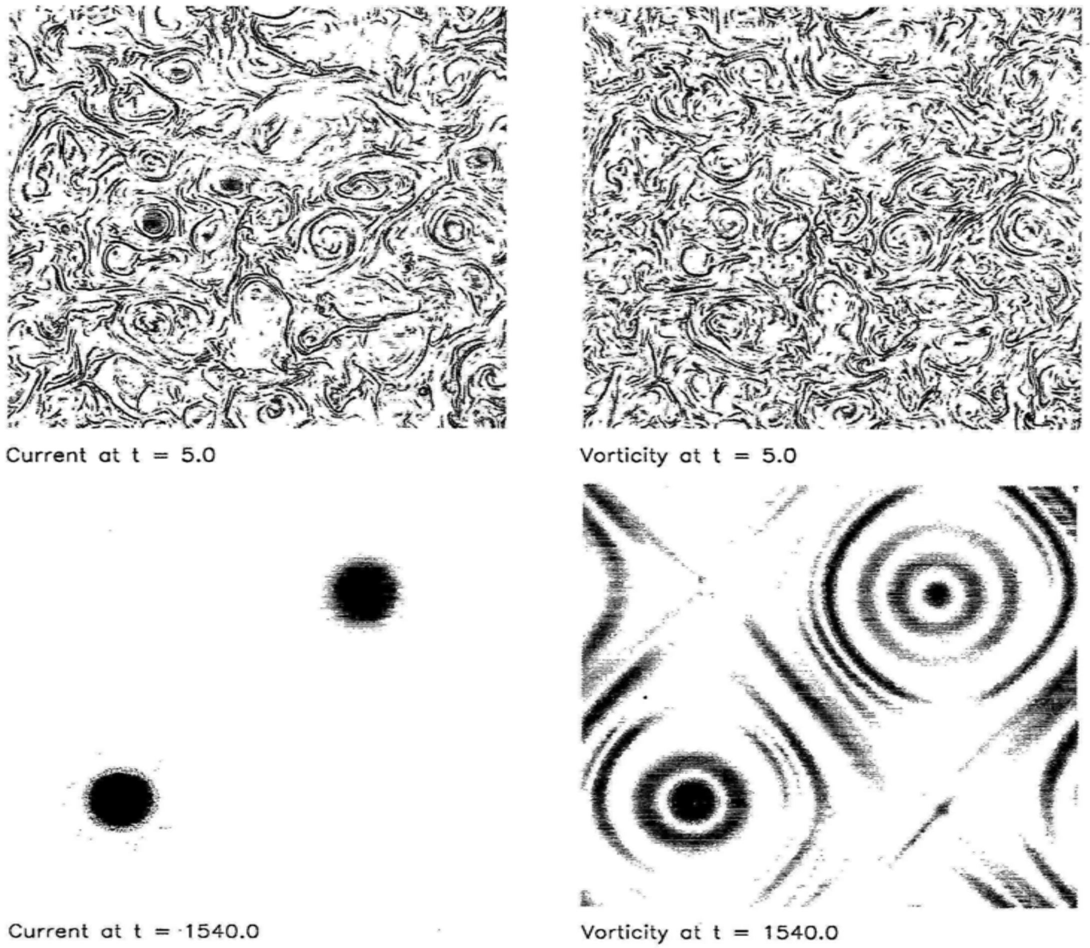

R. Kinney, J.C. McWilliams, T. Tajima
Phys. Plasmas 2 (1995) 3623.

Numerical simulations of the MHD equations.

Compare the two approaches

Conservation eqs.

$$
\begin{aligned}
\frac{\partial n}{\partial t}+\nabla\cdot(n\mathbf{v}) &= 0\\
mn\left(\frac{\partial}{\partial t}+\mathbf{v}\cdot\nabla\right)\mathbf{v} &= -\nabla p-\nabla\cdot\pi+\mathbf{F}\\
\frac{3}{2}n\left(\frac{\partial}{\partial t}+\mathbf{v}\cdot\nabla\right)T &= -\nabla\cdot\mathbf{q}-p\left(\nabla\cdot\mathbf{v}\right)-\pi:\nabla\mathbf{v}+Q
\end{aligned}
$$

Valid for : coffee, ocean, sun.

Lagrangian

$$
\begin{aligned}
\mathcal{L}\left(x^{\mu},\phi^{\nu},\partial_{\rho}\phi^{\nu}\right) &\rightarrow \mathcal{S}=\int dx\,dt\,\mathcal{L}\\
\frac{\partial}{\partial x^{\mu}}\frac{\delta\mathcal{L}}{\delta\left(\frac{\partial\phi^{\nu}}{\partial x^{\mu}}\right)}-\frac{\delta\mathcal{L}}{\delta\phi^{\nu}} &= 0
\end{aligned}
$$

Valid for : a single system.
Just give the initial state.

Lagrangians are preferable. But, how to find a Lagrangian ? See Phys.Rev.

Ideal fluid in $2D$ space (Euler eq.)

$$\frac{d\omega}{dt} = 0 \rightarrow \frac{\partial \nabla_\perp^2 \psi}{\partial t} + \left[\left(-\nabla_\perp \psi \times \widehat{\mathbf{n}} \right) \cdot \nabla_\perp \right] \nabla_\perp^2 \psi = 0$$

At late times of the relaxation process: the *sinh*-Poisson equation

$$\Delta \psi + \gamma \sinh \left(\beta \psi \right) = 0 \tag{1}$$

The Charney-Hasegawa-Mima equation

The equation (CHM) derived for the two-dimensional plasma drift waves and for Rossby waves in meteorology is:

$$\left(\nabla_\perp^2 - 1 \right) \frac{\partial \phi}{\partial t} + \kappa \frac{\partial \phi}{\partial y} + \left[\left(-\nabla_\perp \phi \times \widehat{\mathbf{n}} \right) \cdot \nabla_\perp \right] \nabla_\perp^2 \phi = 0 \tag{2}$$

Equivalence with discrete models

We will try to write Lagrangians *not* directly for fluids and plasmas but for equivalent discrete models.

An equivalent discrete model for the Euler equation

$$\frac{dr_k^i}{dt} = \varepsilon^{ij} \frac{\partial}{\partial r_k^j} \sum_{n=1, n\neq k}^{N} \omega_n G\left(\mathbf{r}_k - \mathbf{r}_n\right) \ , \ i,j = 1,2 \ , \ k = 1, N \tag{3}$$

the Green function of the Laplacian

$$G\left(\mathbf{r}, \mathbf{r}'\right) \approx -\frac{1}{2\pi} \ln\left(\frac{|\mathbf{r} - \mathbf{r}'|}{L}\right) \tag{4}$$

An equivalent discrete model for the CHM equation

The equations of motion for the vortex ω_k at (x_k, y_k) under the effect of the others are

$$-2\pi\omega_k \frac{dx_k}{dt} = \frac{\partial W}{\partial y_k}$$
$$-2\pi\omega_k \frac{dy_k}{dt} = -\frac{\partial W}{\partial x_k}$$

where

$$W = \pi \sum_{\substack{i=1 \\ i\neq j}}^{N} \sum_{j=1}^{N} \omega_i \omega_j K_0 \left(m \left| \mathbf{r}_i - \mathbf{r}_j \right| \right)$$

The Rosette stone, (British Museum) the same message written in three alphabets

Physical model $\rightarrow$ point-like vortices $\rightarrow$ field theory.

The water Lagrangian

2D Euler fluid: Non-Abelian $SU(2)$, Chern-Simons, 4^{th} order

$$\begin{aligned}\mathcal{L} &= -\varepsilon^{\mu\nu\rho} Tr\left(\partial_\mu A_\nu A_\rho + \frac{2}{3} A_\mu A_\nu A_\rho\right) + \\ & iTr\left(\Psi^\dagger D_0 \Psi\right) - \frac{1}{2} Tr\left(\left(D_i \Psi\right)^\dagger D_i \Psi\right) + \frac{1}{4} Tr\left(\left[\Psi^\dagger, \Psi\right]\right)^2\end{aligned} \tag{5}$$

where

$$D_\mu \Psi = \partial_\mu \Psi + \left[A_\mu, \Psi\right]$$

The equations of motion are

$$iD_0 \Psi = -\frac{1}{2}\mathbf{D}^2 \Psi - \frac{1}{2}\left[\left[\Psi, \Psi^\dagger\right], \Psi\right] \tag{6}$$

$$F_{\mu\nu} = -\frac{i}{2}\varepsilon_{\mu\nu\rho} J^\rho \tag{7}$$

The Hamiltonian density is

$$\mathcal{H} = \frac{1}{2} Tr \left((D_i \Psi)^\dagger (D_i \Psi) \right) - \frac{1}{4} Tr \left(\left[\Psi^\dagger , \Psi \right]^2 \right) \tag{8}$$

Using the notation $D_\pm \equiv D_1 \pm i D_2$

$$\begin{aligned} Tr \left((D_i \Psi)^\dagger (D_i \Psi) \right) &= Tr \left((D_- \Psi)^\dagger (D_- \Psi) \right) + \\ & \frac{1}{2} Tr \left(\Psi^\dagger \left[\left[\Psi , \Psi^\dagger \right] , \Psi \right] \right) \end{aligned}$$

Then the energy density is

$$\mathcal{H} = \frac{1}{2} Tr \left((D_- \Psi)^\dagger (D_- \Psi) \right) \geq 0 \tag{9}$$

and the Bogomol'nyi inequality is saturated at *self-duality*

$$D_- \Psi = 0 \tag{10}$$

$$\partial_+ A_- - \partial_- A_+ + [A_+ , A_-] = \left[\Psi , \Psi^\dagger \right] \tag{11}$$

The *static* solutions of the *self-duality* equations

The algebraic *ansatz*:

$$\begin{aligned}
[E_+, E_-] &= H \\
[H, E_\pm] &= \pm 2E_\pm \\
\mathrm{tr}\left(E_+ E_-\right) &= 1 \\
\mathrm{tr}\left(H^2\right) &= 2
\end{aligned} \tag{12}$$

taking

$$\psi = \psi_1 E_+ + \psi_2 E_- \tag{13}$$

and

$$\begin{aligned}
A_x &= \frac{1}{2}\left(a - a^*\right) H \\
A_y &= \frac{1}{2i}\left(a + a^*\right) H
\end{aligned} \tag{14}$$

The gauge field tensor

$$F_{+-} = \left(-\partial_+ a^* - \partial_- a\right) H$$

and from the first self-duality equation

$$\frac{\partial \psi_1}{\partial x} - i \frac{\partial \psi_1}{\partial y} - 2\psi_1 a^* = 0 \tag{15}$$

$$\frac{\partial \psi_2}{\partial x} - i \frac{\partial \psi_2}{\partial y} + 2\psi_2 a^* = 0 \tag{16}$$

and their complex conjugate from $\left(D_- \psi\right)^\dagger = 0$.

Notation : $\rho_1 \equiv \left|\psi_1\right|^2$, $\rho_2 \equiv \left|\psi_2\right|^2$

$$\Delta \ln (\rho_1 \rho_2) = 0 \tag{17}$$

$$\Delta \ln \rho_1 + 2(\rho_1 - \rho_1^{-1}) = 0 \tag{18}$$

We then have

$$\Delta\psi + \gamma \sinh (\beta\psi) = 0. \tag{19}$$

The water we drink is *self-dual*

The Lagrangian of $2D$ *plasma in strong magnetic field: Non-Abelian* $SU(2)$, *Chern-Simons*, 6^{th} *order*

- gauge field, with "potential" A^{μ}, ($\mu = 0, 1, 2$ for (t, x, y)) described by the Chern-Simons Lagrangean;
- matter ("Higgs" or "scalar") field ϕ described by the covariant kinematic Lagrangean (*i.e.* covariant derivatives, implementing the minimal coupling of the gauge and matter fields)
- matter-field self-interaction given by a potential $V\left(\phi, \phi^{\dagger}\right)$ with 6^{th} power of ϕ;
- the matter and gauge fields belong to the *adjoint* representation of the algebra $SU(2)$

$$\begin{aligned}\mathcal{L} &= -\kappa\varepsilon^{\mu\nu\rho}\mathrm{tr}\left(\partial_\mu A_\nu A_\rho + \frac{2}{3}A_\mu A_\nu A_\rho\right) \\ &-\mathrm{tr}\left[\left(D^\mu\phi\right)^\dagger\left(D_\mu\phi\right)\right] \\ &-V\left(\phi,\phi^\dagger\right)\end{aligned} \tag{20}$$

Sixth order potential

$$V\left(\phi,\phi^\dagger\right) = \frac{1}{4\kappa^2}\mathrm{tr}\left[\left(\left[\left[\phi,\phi^\dagger\right],\phi\right] - v^2\phi\right)^\dagger\left(\left[\left[\phi,\phi^\dagger\right],\phi\right] - v^2\phi\right)\right]. \tag{21}$$

The Euler Lagrange equations are

$$D_\mu D^\mu \phi = \frac{\partial V}{\partial \phi^\dagger} \tag{22}$$

$$-\kappa\varepsilon^{\nu\mu\rho}F_{\mu\rho} = iJ^\nu \tag{23}$$

The energy can be written as a sum of squares. The *self-duality* eqs.

$$\begin{aligned} D_-\phi &= 0 \\ F_{+-} &= \pm\frac{1}{\kappa^2}\left[v^2\phi - \left[\left[\phi,\phi^\dagger\right],\phi\right],\phi^\dagger\right] \end{aligned} \tag{24}$$

The algebraic *ansatz* : in the Chevalley basis

$$\begin{aligned} [E_+,E_-] &= H \\ [H,E_\pm] &= \pm 2E_\pm \\ \mathrm{tr}\,(E_+E_-) &= 1 \\ \mathrm{tr}\,\left(H^2\right) &= 2 \end{aligned} \tag{25}$$

The fields

$$\phi = \phi_1 E_+ + \phi_2 E_-$$

$$A_+ = aH, A_- = -a^* H$$

Equations for the components of the density of vorticity (here for $'+'$)

$$-\frac{1}{2}\Delta \ln \rho_1 = -\frac{1}{\kappa^2}(\rho_1-\rho_2)\left[2(\rho_1+\rho_2)-v^2\right] \tag{26}$$

$$-\frac{1}{2}\Delta \ln \rho_2 = \frac{1}{\kappa^2}(\rho_1-\rho_2)\left[2(\rho_1+\rho_2)-v^2\right] \tag{27}$$

$$\Delta \ln(\rho_1\rho_2) = 0$$

introduce a single variable

$$\rho \equiv \frac{\rho_1}{v^2/4} = \frac{v^2/4}{\rho_2} \tag{28}$$

and obtain

$$-\frac{1}{2}\Delta \ln \rho = -\frac{1}{4}\left(\frac{v^2}{\kappa}\right)^2\left(\rho-\frac{1}{\rho}\right)\left[\frac{1}{2}\left(\rho+\frac{1}{\rho}\right)-1\right] \tag{29}$$

The energy at Self-Duality for two choices of the Bogomolnyi form for the action functional

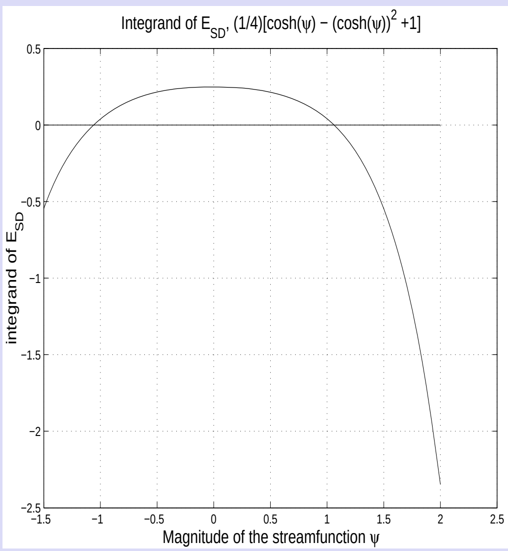

$$\Delta\psi - \sinh\psi\,(\cosh\psi - 1) = 0$$

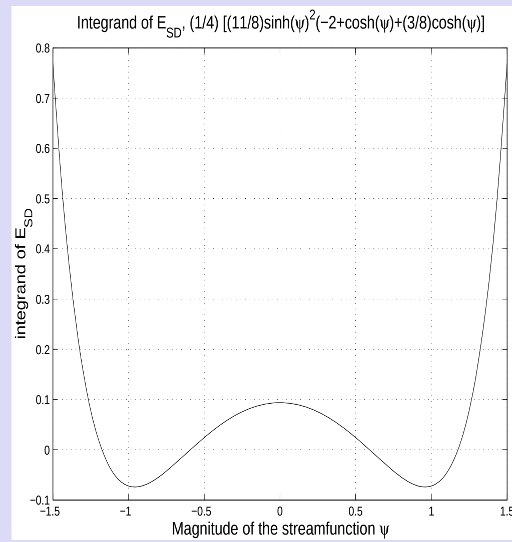

$$\Delta\psi + \frac{1}{2}\sinh\psi\,(\cosh\psi - 1) = 0$$

This simplest form of the equation governing the stationary states of the CHM eq.

$$\Delta\psi + \frac{1}{2}\sinh\psi\,(\cosh\psi - 1) = 0$$

The 'mass of the photon' is

$$m = \frac{v^2}{\kappa} = \frac{1}{\rho_s}$$

$$\begin{aligned} \kappa &\equiv c_s \\ v^2 &\equiv \Omega_{ci} \end{aligned}$$

Half-way Conclusions

The field theoretical formalism provides interesting results:

- identifies preferred states as extrema of an action functional
- derives explicit differential equations for these states
- allows to investigate neighboring states and reveals the existence of cuasi-degenerate directions and multiple minima of the action in the function space
- reveals the universal nature of the extrema, as self-dual states
- practical applications

The FT model still has to be examined:

It needs a clear mapping: "formalism" - "physics"
It needs better investigation of the equations of motion
It invites to study the natural extension of the theory.

Integration of the differential equation

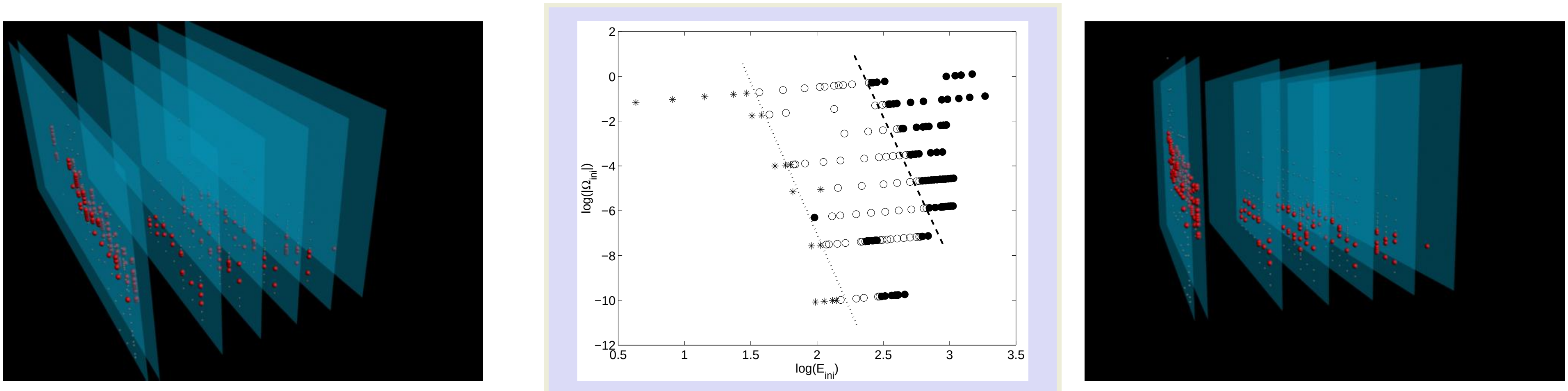

Figure 1: The structure of the space of initial conditions. The successful (coherent vortex) solutions are shown as red dots.

Solutions: trivial, turbulent, coherent, strongly concentrated.

Comparison with experiment

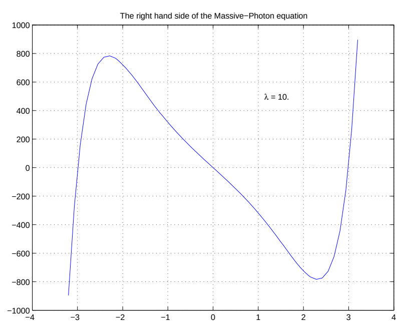

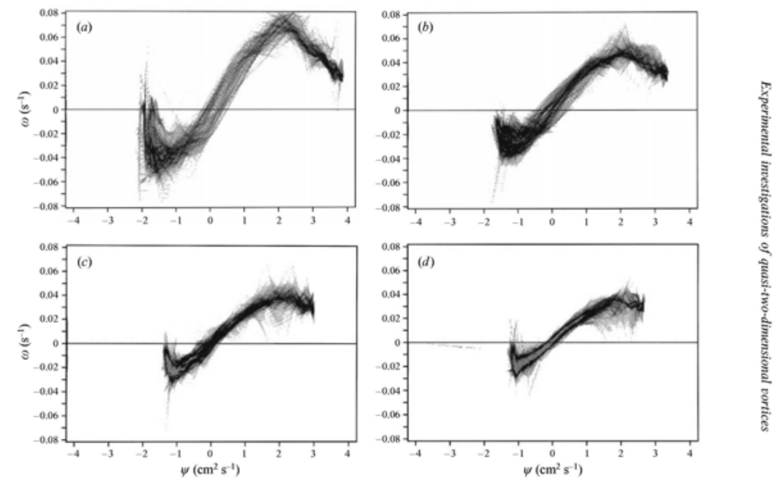

FIGURE 21. (ω, ψ) scatter plots of the decaying vorticity field in Exp. 17, at (a) 1 min, (b) 5 min, (c) 10 min, and (d) 15 min after switching off the forcing. The (ω, ψ)-values of all points on a grid in physical space, with a mesh size of approximately $(1\ mm)^2$, are plotted.

Experimental Investigation of quasi-two-dimensional in a stratified fluid with source-sink forces
Frans de Rooij, P.F. Linden, S.P. Dalziel, Journal of Fluid Mechanics **383** (1999) 249.

Figure 2: The pair (ψ, ω) and the experiment (ω is negative).

Comparison with numerical simulations in the asymptotic regime

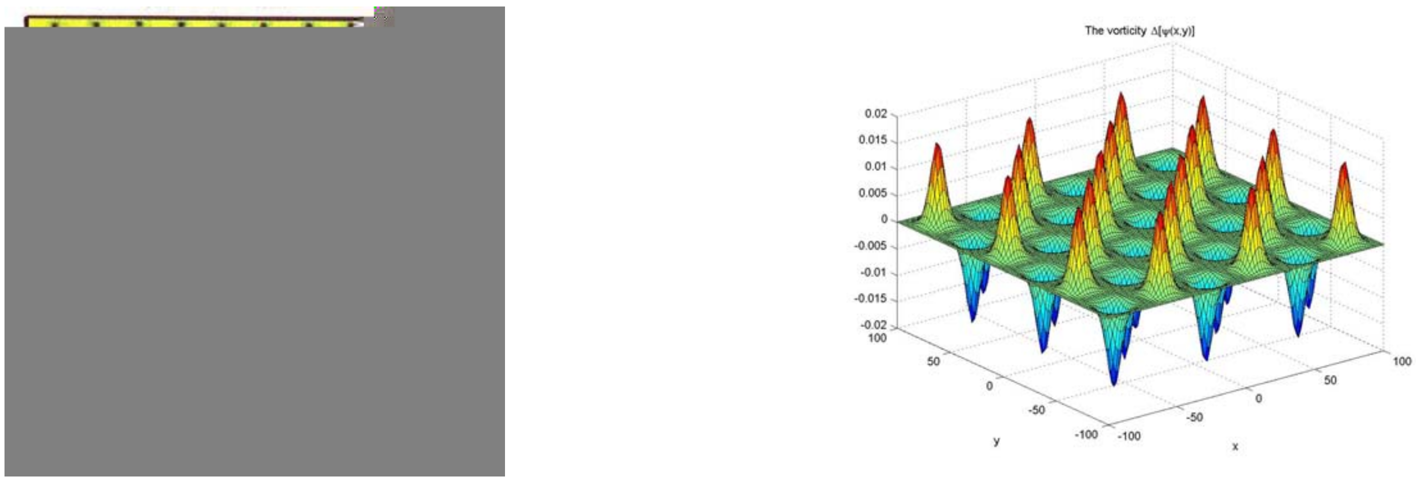

Figure 3: Comparison between numerical calculation of the CHM stationary states (Khukharin 2002) and solution of the Equation (1).

Periodic structure of vortices.

Applications

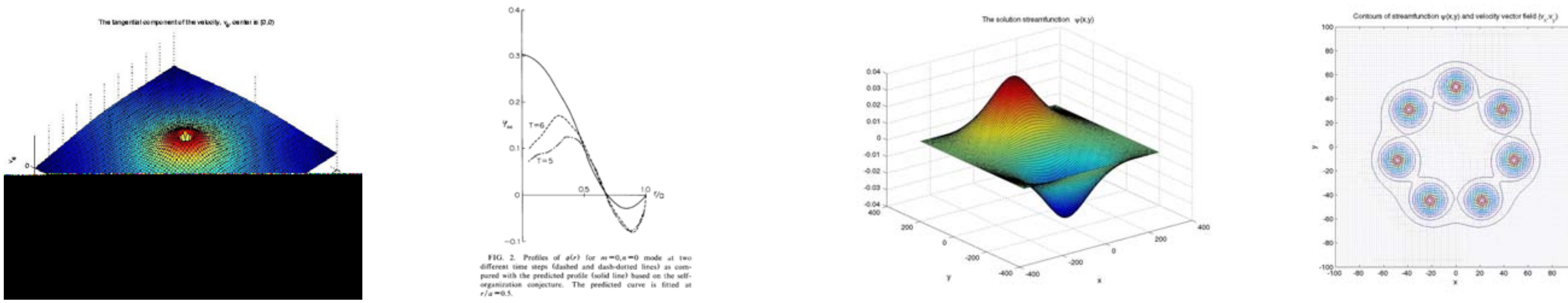

Figure 4: The atmospheric vortex, the plasma vortex, the flows in tokamak,the crystal of vortices in non-neutral plasma.

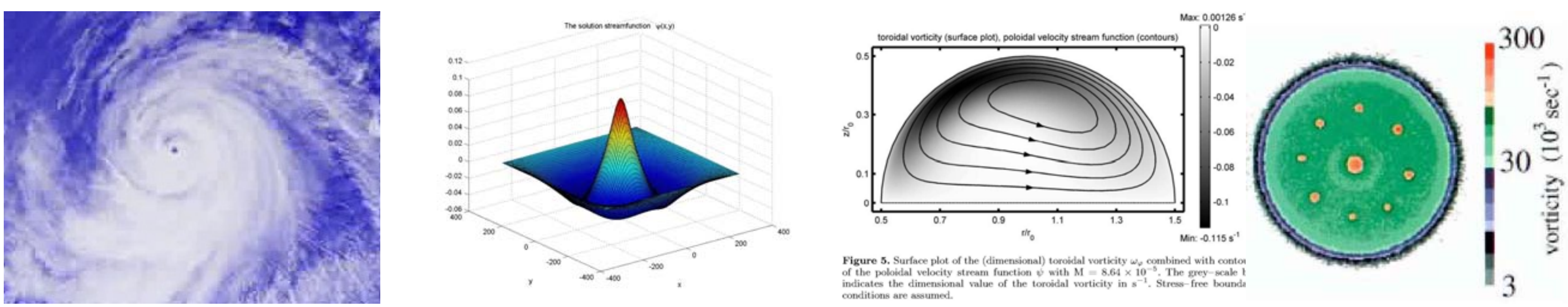

The tropical cyclone

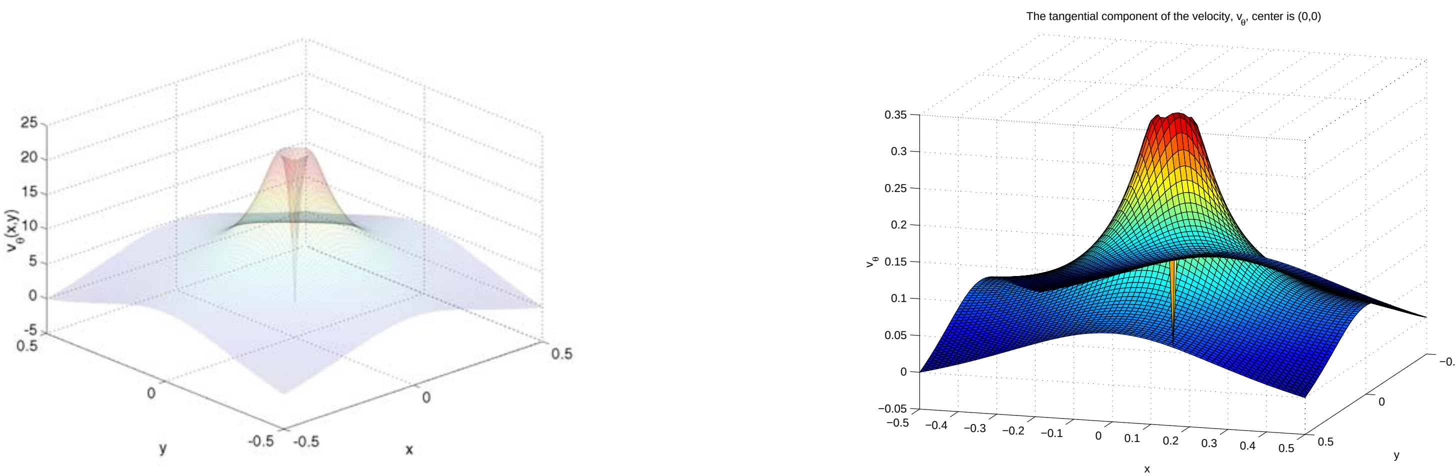

Figure 5: The tangential component of the velocity, $v_\theta(x,y)$

This is an atmospheric vortex.

The tropical cyclone , comparisons

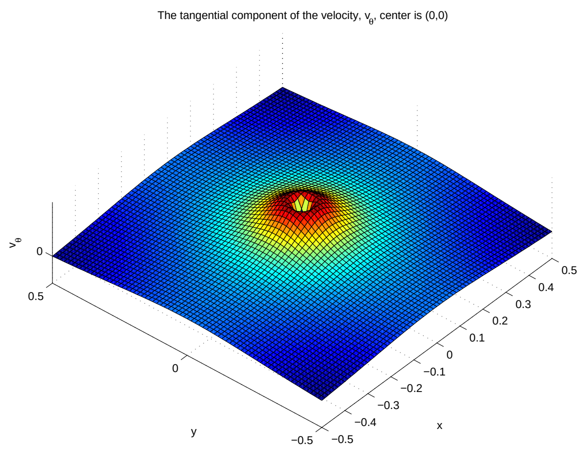

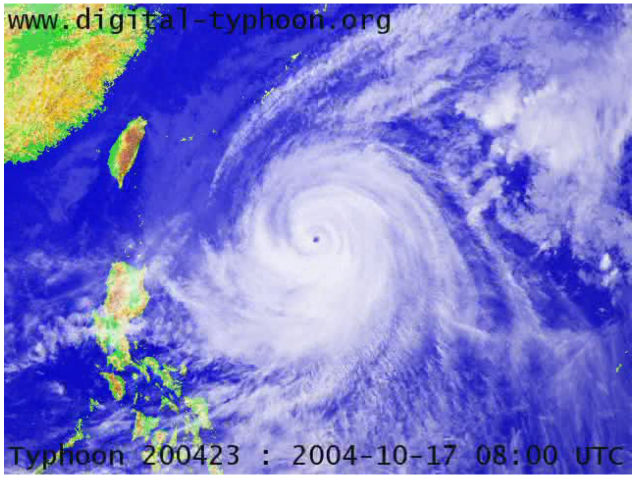

Figure 6: The solution and the image from a satelite.

The solution reproduces the *eye* radius, the radial extension and the vorticity magnitude.

Scaling relationships between main parameters of the tropical cyclone eye-wall radius, maximum tangential wind, maximum radial extension

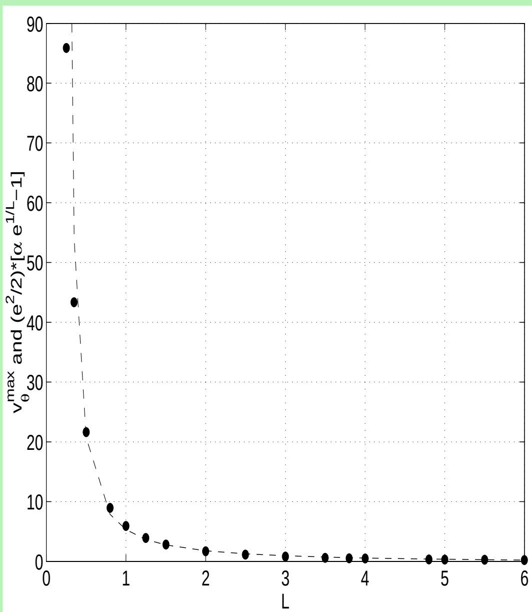

$$v_{\theta}^{\max}(L) \simeq \frac{e^2}{2}\left[\alpha \exp\left(\frac{\sqrt{2}}{R_{\max}}\right) - 1\right]$$

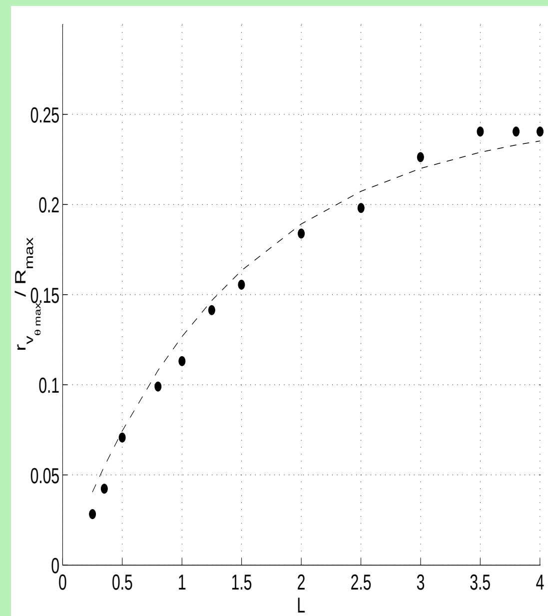

$$\frac{r_{v_{\theta}^{max}}}{R_{max}} = \frac{1}{4}\left[1 - \exp\left(-\frac{R_{max}}{2}\right)\right]$$

Few *remarkable* hurricanes

Table 1: Comparison between calculated and respectively observed magnitudes of the maximum tangential wind for four cases of tropical cyclones

Name	Input (obs)		Calculated			Observed
	$R_{\max}^{phys}$ (km)	$\frac{r_{v_\theta^{\max}}}{R_{\max}}$	L	Rossby ρ_g (km)	$(v_\theta^{\max})$ (m/s)	$(v_\theta^{\max})$ (m/s)
Andrew	120	0.1	0.72	117.85	64.31	68
Katrina	300	0.111	0.83	212	88.6	77.8
Rita	350	0.125	0.98	252.47	77.5	77.8
Diana	160	0.1125	0.845	133.81	56.86	55

(*Comment ne pas perdre la tête?*)

Profile of the azimuthal wind velocity $v_\theta(r)$

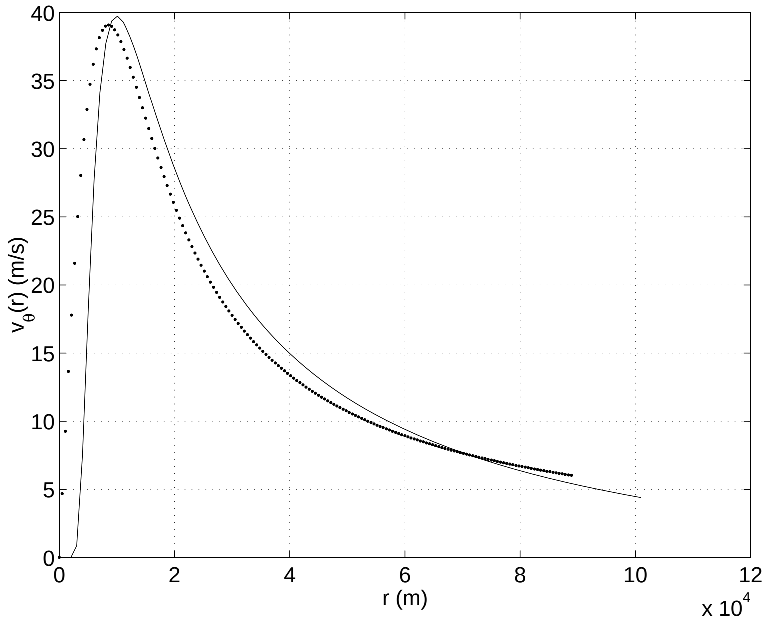

Comparison between the Holland's empirical model for v_θ (continuous line) and our result (dotted line).

Tokamak plasma. Solution for $L = 307$: mono- and multipolar vortex

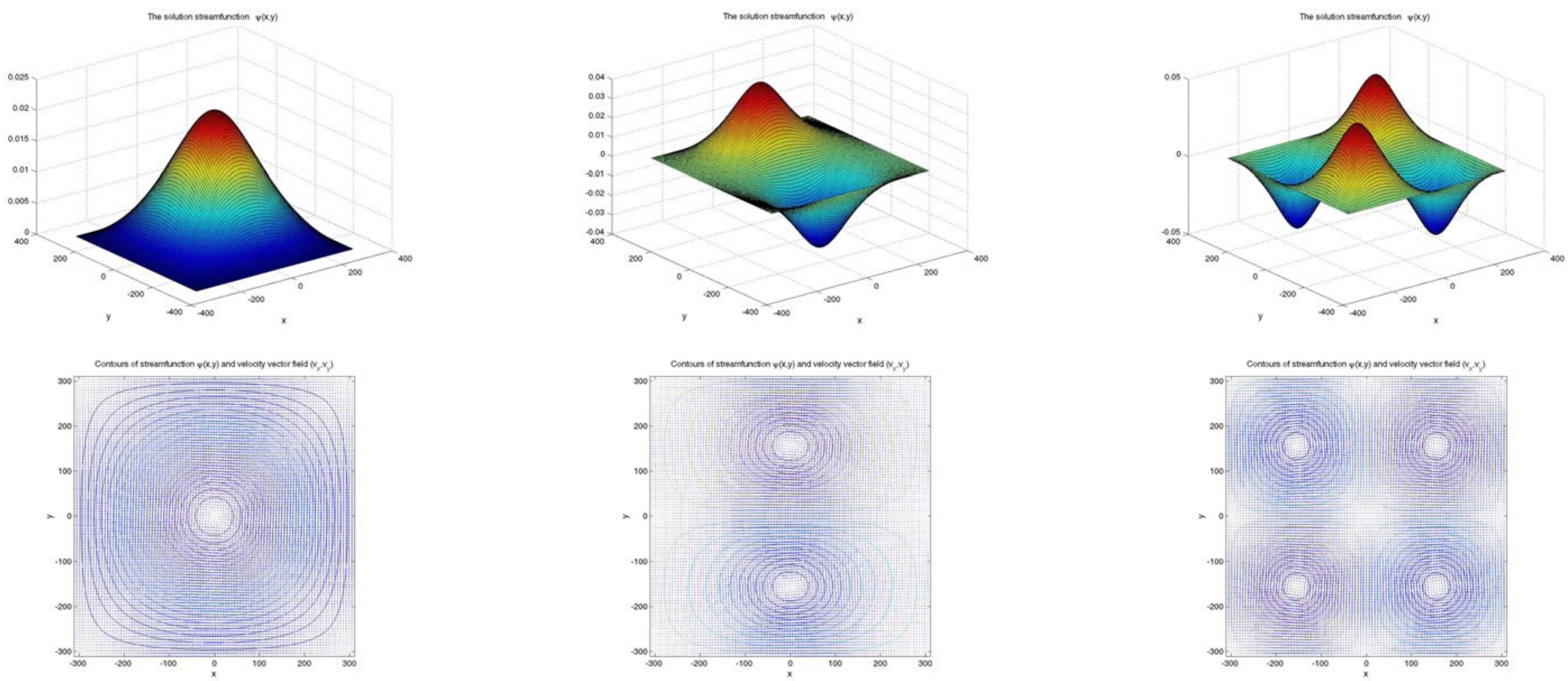

Self-organisation of the drift turbulence (Wakatani-Hasegawa)

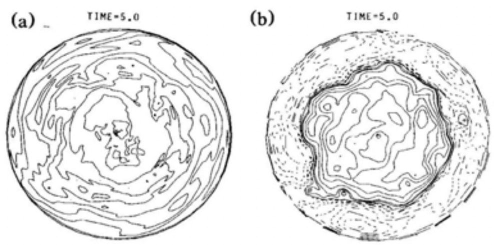

FIG. 1. (a) The density contour and (b) the potential contour from the three-dimensional computer simulation of electrostatic plasma turbulence in a cylindrical plasma with magnetic curvature and shear. In (b) the solid (dashed) lines are for the positive (negative) potential contours. Note the development of closed potential contours near the $\phi \simeq 0$ surface.

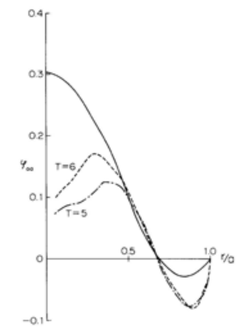

FIG. 2. Profiles of $\phi(r)$ for $m=0, n=0$ mode at two different time steps (dashed and dash-dotted lines) as compared with the predicted profile (solid line) based on the self-organization conjecture. The predicted curve is fitted at $r/a=0.5$.

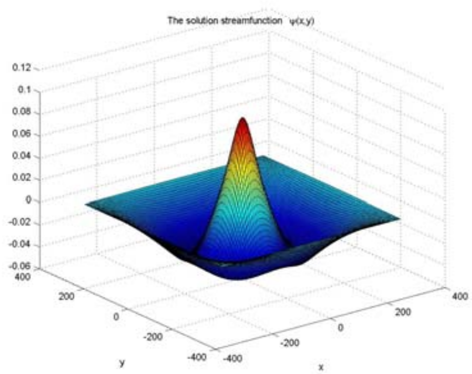

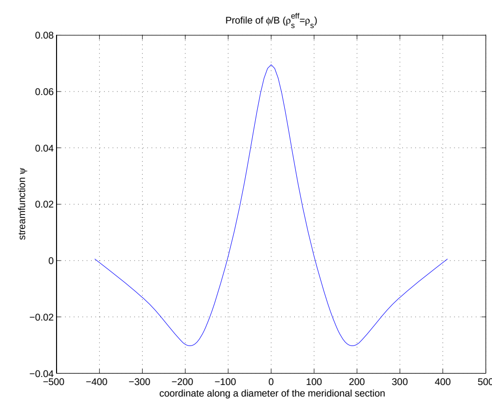

The crystals of plasma vortices

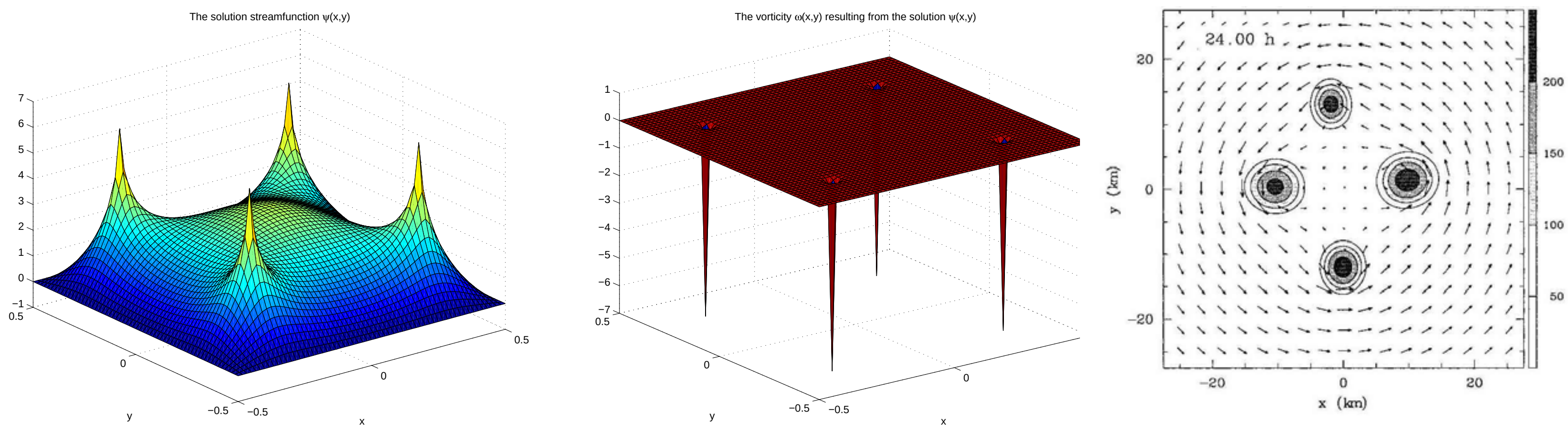

Figure 7: The crystals of plasma vortices.

Comparisons of crystal-type solutions with experiment.

Vortex crystals in non-neutral plasma

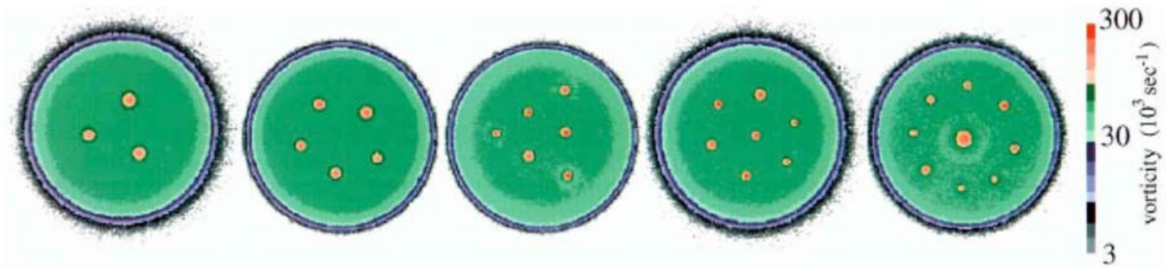

FIG. 1. Vortex crystals observed in magnetized electron columns (Ref. 8). The color map is logarithmic. This figure shows vortex crystals with (from left to right) $M=3$, 5, 6, 7, and 9 intense vortices immersed in lower vorticity backgrounds. In a vortex crystal equilibrium, the entire vorticity distribution $\zeta(r,\theta)$ is stationary in a rotating frame; i.e., ζ is a function of the variable $-\psi+\frac{1}{2}\Omega r^2$, where ψ is the stream function and Ω is the frequency of the rotating frame.

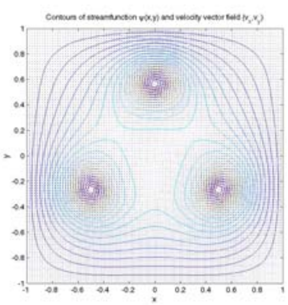

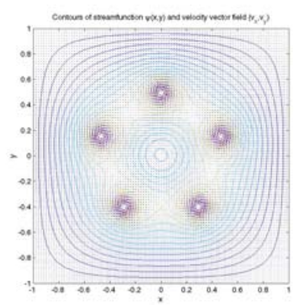

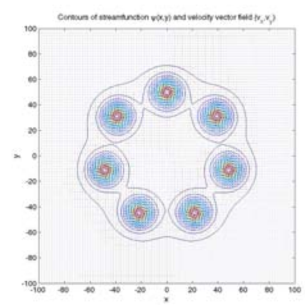

Comparison of our vortex solution with experiment.

Laser generated plasma

330 Mourou, Tajima, and Bulanov:

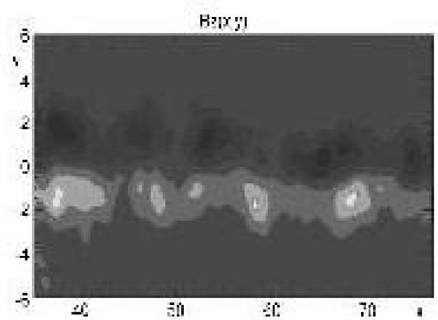

FIG. 18. Vortex row behind the laser pulse seen in the isocontours of the magnetic field.

Figure 8: Structure of the magnetic field in a plasma generated by a strong Laser pulse. The equation for B has the same nonlinear form as the CHM equation.

Filamentation in Laser-generated plasmas (for Inertial Fusion)

The equation for the magnetic field generated in a laser-driven plasma

$$\begin{aligned}
& \frac{1}{\mu_0 e n_0} \frac{\partial}{dt} \nabla^2 B + \left(\frac{1}{\mu_0 e n_0} \right)^2 \left[\left(-\widehat{\mathbf{e}}_z \times \nabla B \right) \cdot \nabla \right] \nabla^2 B \\
= \quad & \frac{\partial B}{\partial t} + \frac{1}{\mu_0 e n_0^2} \left[\left(-\widehat{\mathbf{e}}_z \times \nabla n_0 \right) \cdot \nabla \right] \nabla^2 n_0 \\
& + \frac{1}{e n_0} \left[\left(-\widehat{\mathbf{e}}_z \times \nabla n_0 \right) \cdot \nabla \right] \nabla^2 T_1
\end{aligned}$$

where T_1 is the perturbed temperature

$$\frac{\partial T_1}{\partial t} + T_0 \left[(\gamma - 1) \frac{n_0'}{n_0} - \frac{T_0'}{T_0} \right] \frac{\partial B}{\partial y} = - \left[\left(-\widehat{\mathbf{e}}_z \times \nabla B \right) \cdot \nabla \right] \nabla^2 T_1$$

When the T_1 perturbation and the *scalar nonlinearity* $B \partial B / \partial y$ can be neglected, the equation for B becomes the classical CHM-type equation.

A sheet of current is broken up into filaments.

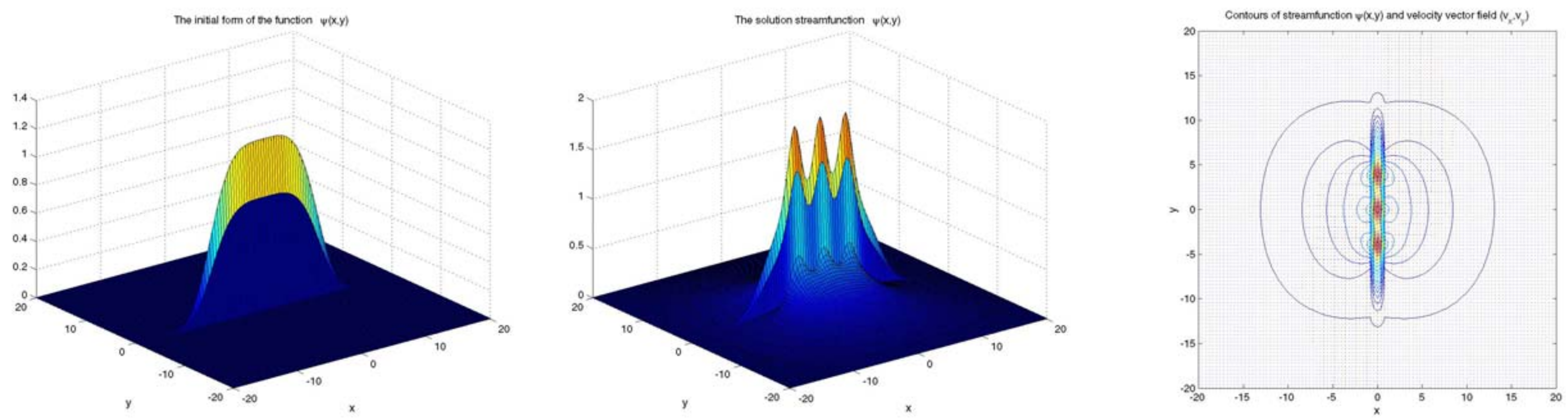

Figure 9: Filamentation in a current sheet.

Current sheet.

Final Conclusions

It seems it works.

- Hamlet: *The rest is silance*
- Einsetin: *The rest is details*
- (Field Theory Book): *The rest is gauge*

Save your work.

Prepare for shutdown.

Articles

- F. Spineanu and M. Vlad, Phys. Rev. Letters, **94** (2005) 235003.
- F. Spineanu and M. Vlad, Phys. Rev. E 67 (2003) 046309
- F. Spineanu and M. Vlad, arXiv.org/physics/0503155
- F. Spineanu and M. Vlad, arXiv.org/physics/0501020
- F. Spineanu and M. Vlad, arXiv.org/physics/0909.2583
- F. Spineanu and M. Vlad, arXiv.org/physics/1001.0151
- F. Spineanu and M. Vlad, Geophysical and Astrophysical Fluid Dynamics **103**, (2009) 223.